

REGULAR PAPERS

Electrical properties of Al foil/n-4H-SiC Schottky junctions fabricated by surface-activated bonding

To cite this article: Sho Morita *et al* 2018 *Jpn. J. Appl. Phys.* **57** 02BE01

View the [article online](#) for updates and enhancements.

Related content

- [Effects of annealing on the electrical characteristics of GaAs/GaAs junctions by surface-activated bonding](#)
Li Chai, Jianbo Liang and Naoteru Shigekawa
- [Modulation of electrical properties in Cu/n-type InP Schottky junctions using oxygen plasma treatment](#)
Hogyoung Kim, Yunae Cho, Chan Yeong Jung *et al.*
- [Temperature dependence of barrier height in Ni/n-GaN Schottky barrier diode](#)
Takuya Maeda, Masaya Okada, Masaki Ueno *et al.*



Electrical properties of Al foil/n-4H-SiC Schottky junctions fabricated by surface-activated bonding

Sho Morita¹, Jianbo Liang¹, Moeko Matsubara², Marwan Dhamrin², Yoshitaka Nishio², and Naoteru Shigekawa^{1*}

¹Graduate School of Engineering, Osaka City University, Osaka 558-8585, Japan

²Core Technology Center, Toyo Aluminium K.K., Osaka 541-0056, Japan

*E-mail: Shigekawa@elec.eng.osaka-cu.ac.jp

Received July 22, 2017; accepted September 4, 2017; published online November 30, 2017

We fabricate 17- μm -thick Al foil/n-4H-SiC Schottky junctions by surface-activated bonding. Their current–voltage and capacitance–voltage characteristics are compared with those of Schottky junctions fabricated by evaporating Al layers on n-4H-SiC epilayers. We find that the ideality factor of Al foil/SiC junctions is larger than that of conventional junctions, which is due to the irradiation of the fast atom beam (FAB) of Ar. The ideality factor of Al foil/SiC junctions is improved by annealing at 400 °C. We also find that the Schottky barrier height is increased by FAB irradiation, which is likely to be due to the negative charges formed at SiC surfaces. © 2018 The Japan Society of Applied Physics

1. Introduction

4H-SiC has the potential as vital parts of low-loss, high-temperature, high-frequency, and high-power devices owing to its superior electrical and physical properties.^{1–3} Recently, SiC power devices and modules have become available in the market. The advantages of SiC, however, have not yet been fully exploited in these devices and modules. New technologies for soldering and attaching dies such as nano- or microparticle pastes or solders have been explored so as to realize their operations at high temperatures.^{4–7} Interconnections with lower parasitic inductances have also been investigated.^{8,9}

Using surface-activated bonding (SAB) technologies,^{10,11} dissimilar materials are firmly attached to each other after their surfaces are irradiated with the fast atom beam (FAB) of noble gases such as Ar. Various junctions such as Si/GaAs,^{12,13} Al/Al,^{14,15} Cu/Cu,^{16,17} Si/SiC,^{18,19} and Al/Si²⁰ systems were reportedly fabricated by SAB. These junctions were applied to solar cells, three-dimensional integration, packaging, and new power devices. We previously fabricated InGaP/GaAs/Si²¹ triple-junction solar cells and 4H-SiC/Si²² heterojunction bipolar transistors by SAB.

Al has widely been used for contacts and interconnections in semiconductor devices and circuits owing to its low resistivity. The thickness of Al films fabricated by conventional methods such as evaporation, sputtering, and electroplating determines the period of process and hence the cost. Such Al films, consequently, may not be useful for interconnects in power devices and modules that are required to handle large electric powers. On the assumption that ultrathick metal junctions on semiconductors could provide a solution for this problem, we previously fabricated Al foil/Si junctions by SAB and examined their possibility as contacts and interconnects.²³ We have recently found that Al foils bonded on n-4H-SiC layers worked as Schottky contacts.²⁴ In this paper, we examine the electrical properties of Al foil/4H-SiC junctions in comparison with Schottky junctions fabricated by evaporating Al films with the emphasis on the effects of annealing. Junctions fabricated by evaporation after irradiating the surfaces of SiC layers with the FAB of Ar are also characterized.

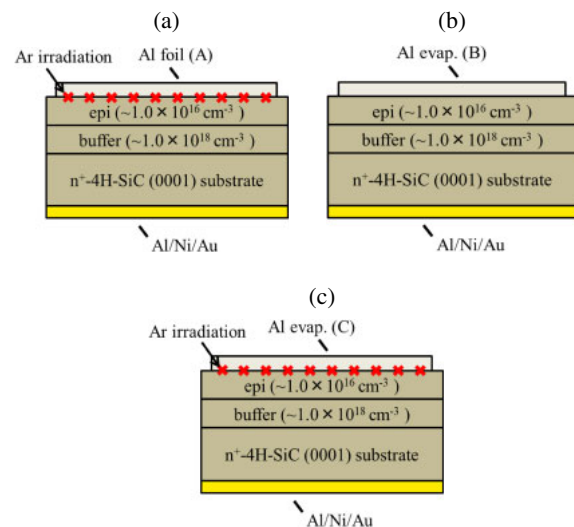


Fig. 1. (Color online) Schematic cross sections of Junctions (a) (A), (b) (B), and (c) (C).

2. Experimental methods

We prepared SiC epitaxial substrates by successively growing 0.3- μm -thick n⁺-doped buffer layers ($1 \times 10^{18} \text{ cm}^{-3}$) and 6- μm -thick n-doped ($1 \times 10^{16} \text{ cm}^{-3}$) layers on n⁺-doped 4H-SiC(0001) substrates. Ohmic contacts were formed on the back sides of SiC substrates by evaporating Al/Ni/Au multilayers and annealing at 1000 °C for 1 min in N₂ ambient. Then, 17- μm -thick Al foils were bonded to the surfaces of SiC epitaxial substrates by SAB. A Schottky junction, or Junction (A), was obtained by the photolithography and wet etching of the Al foils.

We also fabricated a conventional Al/SiC Schottky junction, or Junction (B), by evaporating Al/Ni/Au multilayers and the lift-off process. In addition, we fabricated another type of Schottky junction, Junction (C), by evaporating the multilayers after irradiating the surfaces of SiC epitaxial substrates with the FAB. The FAB irradiation conditions in preparing Junctions (A) and (C) were similar to those in our previous work.²³ The schematic cross sections of the respective junctions are shown in Fig. 1.

The current–voltage (*I*–*V*) and capacitance–voltage (*C*–*V*) characteristics of the as-prepared junctions were measured at

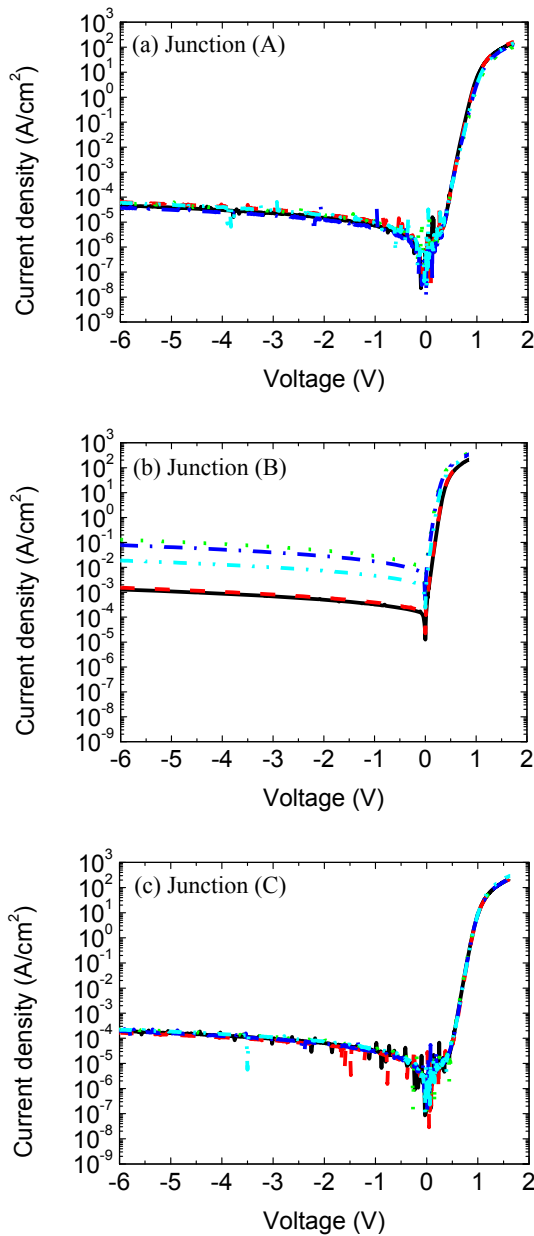


Fig. 2. (Color online) I - V characteristics of five devices of Junctions (a) (A), (b) (B), and (c) (C).

room temperature by using an Agilent B20982A and an Agilent E4980A, respectively. These characteristics were also measured after the junctions were annealed at 400 °C for 1 min in N_2 ambient. In addition, the dependences of the I - V characteristics on the ambient temperature were measured after annealing.

3. Results

3.1 Characteristics before annealing

The I - V characteristics of five devices of the respective junctions are shown in Figs. 2(a)–2(c). Figure 2(b) shows that the I - V curves of Junction (B), or a junction without the FAB irradiation, were largely scattered. The uniformity of I - V curves, however, was improved by FAB irradiation as is seen in Figs. 2(a) and 2(c). Here, we assumed that, among the I - V characteristics shown in Fig. 2(b), the curve with the lowest reverse-bias current represented the intrinsic properties of Junction (B). We compared such characteristics of

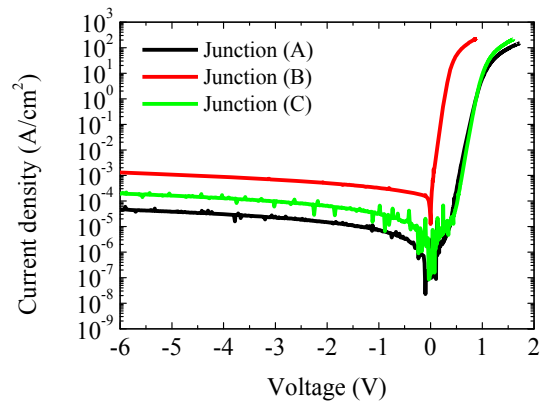


Fig. 3. (Color online) I - V characteristics of the three junctions.

Table I. The parameters characterizing the respective I - V curves are summarized.

	Junction (A)	Junction (B)	Junction (C)
Turn-on voltage (V) (before annealing)	0.65	0.12	0.69
Turn-on voltage (V) (after annealing at 400 °C)	0.59	0.28	0.61
Ideality factor (before annealing)	1.53	1.24	1.47
Ideality factor (after annealing at 400 °C)	1.31	1.21	1.28
Reverse-bias current at -6 V (A/cm ²) (before annealing)	4.6×10^{-5}	1.3×10^{-3}	2.0×10^{-4}
Reverse-bias current at -6 V (A/cm ²) (after annealing at 400 °C)	5.9×10^{-6}	6.5×10^{-5}	6.7×10^{-6}

Junction (B) with typical I - V characteristics of Junctions (A) and (C) in Fig. 3. The turn-on voltage, which we defined as the forward-bias voltage corresponding to the current 10^{-2} A/cm², was determined to be 0.65, 0.12, and 0.69 V for Junctions (A), (B), and (C), respectively. The ideality factors, which were obtained by fitting the characteristics for the forward-bias voltages, were 1.53, 1.24, and 1.47 for Junctions (A), (B), and (C), respectively. The reverse-bias currents at -6 V were 4.6×10^{-5} [Junction (A)], 1.3×10^{-3} [Junction (B)], and 2.0×10^{-4} A/cm² [Junction (C)]. In addition, humps due to recombination were apparent for forward-bias voltages of ~ 0.4 V in the I - V characteristics of Junctions (A) and (C). The parameters characterizing the respective I - V curves are shown in Table I.

The $1/C^2$ - V characteristics of the respective samples measured at 100 kHz are shown in Fig. 4. We confirmed that the concentration of impurities in the n-doped SiC layer was $(6.9\text{--}8.4) \times 10^{15}$ cm⁻³, which was close to the nominal concentration of dopants (1×10^{16} cm⁻³), from the slope of the $1/C^2$ - V curves. The flat-band voltage was found to be 1.10, 0.60, and 1.15 V for Junctions (A), (B), and (C), respectively. These values corresponded to the SBHs of 1.31 [Junction (A)], 0.81 [Junction (B)], and 1.36 eV [Junction (C)], respectively, by assuming that the Fermi level in the n-doped SiC layer was below its conduction band minimum

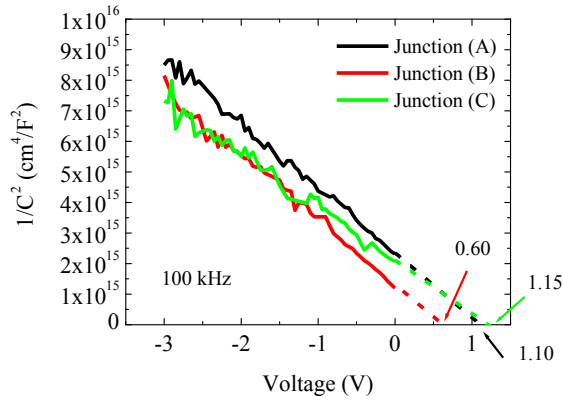


Fig. 4. (Color online) $1/C^2$ - V characteristics of the three junctions.

Table II. SBHs from $1/C^2$ - V characteristics and Richardson's plot (in eV).

	Junction (A)	Junction (B)	Junction (C)
$1/C^2$ - V characteristics (before annealing)	1.31	0.81	1.36
$1/C^2$ - V characteristics (after annealing at 400 °C)	1.37	0.98	1.28
Richardson's plot	0.84	0.66	0.89

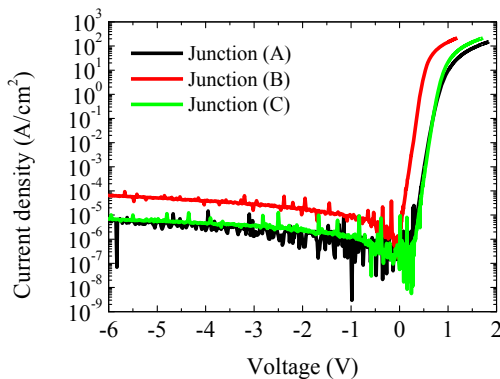


Fig. 5. (Color online) I - V characteristics of the three junctions after annealing at 400 °C.

by 0.21 eV. We found that the SBHs and turn-on voltages correlated with each other. The SBHs of the respective samples are shown in Table II.

3.2 Characteristics after 400 °C annealing

The I - V characteristics of the three junctions after annealing are shown in Fig. 5. The turn-on voltage, ideality factor, and reverse-bias current at -6 V were 0.59 V, 1.31, and 5.9×10^{-6} A/cm², respectively, for Junction (A). They were 0.28 V, 1.21, and 6.5×10^{-5} A/cm² for Junction (B), and 0.61 V, 1.28, and 6.7×10^{-6} A/cm² for Junction (C), respectively. The parameters characterizing the respective I - V curves are also shown in Table I. The ideality factors and reverse-bias characteristics of the respective samples were improved by annealing. The humps were less pronounced in the I - V characteristics of Junctions (A) and (C) after annealing.

The I - V characteristics under forward bias voltages at various temperatures between room temperature and 200 °C are shown in Figs. 6(a)–6(c). We obtained the saturation

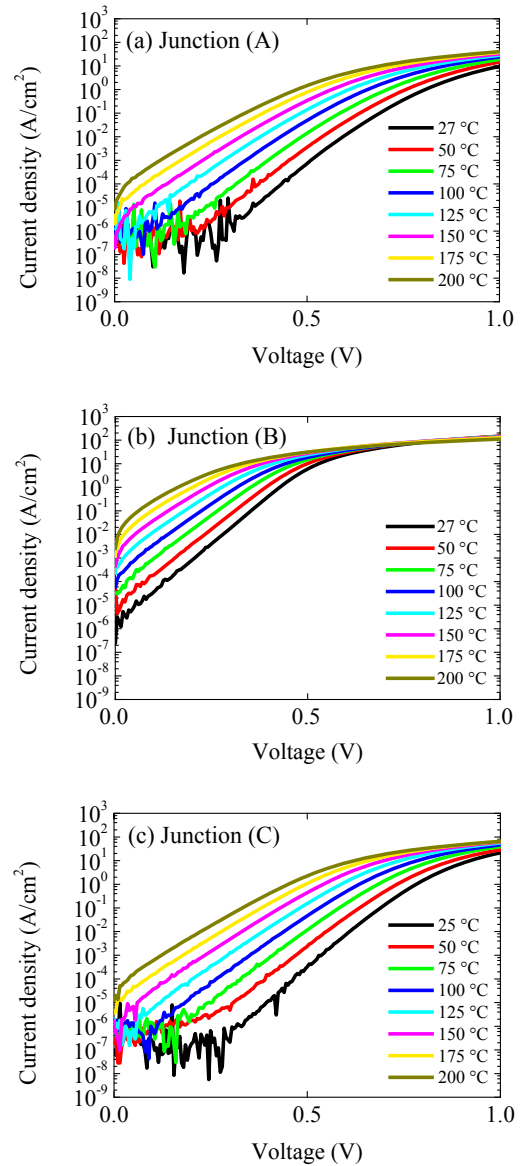


Fig. 6. (Color online) I - V characteristics under forward-bias voltages of Junctions (a) (A), (b) (B), and (c) (C) measured at various temperatures.

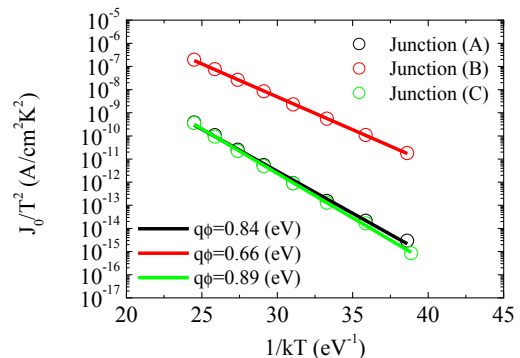


Fig. 7. (Color online) Richardson's plot $\ln(J_0/T^2)$ vs $1/kT$ for the three junctions.

current $J_0 = \lim_{V \rightarrow 0+} J(V)$ by least-squares fitting at each temperature. The relationship between $\ln(J_0/T^2)$ and $1/kT$, or Richardson's plot, is shown in Fig. 7. We found that $\ln(J_0/T^2)$ almost linearly depended on $1/T$. The SBH, which was estimated from the slope of the relationship, was

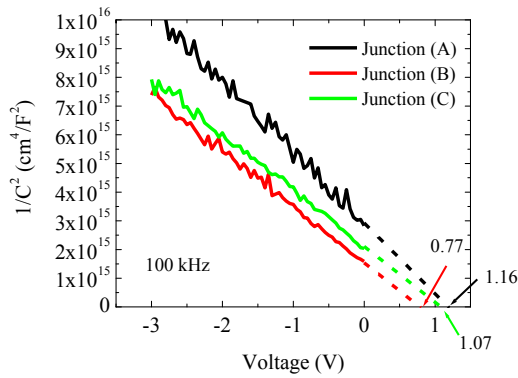


Fig. 8. (Color online) $1/C^2$ - V characteristics of the three junctions after annealing at 400 °C.

determined to be 0.84, 0.66, and 0.89 eV for Junctions (A), (B), and (C), respectively. These results are summarized in Table II.

The $1/C^2$ - V characteristics of the respective junctions are shown in Fig. 8. The flat-band voltages of Junctions (A), (B), and (C) were found to be 1.16, 0.77, and 1.07 V, which corresponded to the SBHs of 1.37, 0.98, and 1.28 eV, respectively. The SBHs of the respective samples are also shown in Table II.

4. Discussion

As is seen from Table I, among the three types of junctions, the ideality factors of Junctions (A) and (C) were larger (worse) than that of Junction (B). This result indicates that traps were introduced on the surfaces of n-SiC layers during FAB irradiation. This view is consistent with the occurrence of humps in the I - V characteristics of Junctions (A) and (C) before annealing.

By annealing at 400 °C, the ideality factors were improved, the humps for Junctions (A) and (C) were not observed, and the reverse-bias currents of the respective junctions were lowered. These results suggest that the impact of FAB irradiation was slightly recovered by annealing.

Table II shows that the SBH extracted from Richardson's plot was smaller than that obtained from the $1/C^2$ - V characteristics by ~ 0.3 – 0.5 eV. Similar results are often obtained in Schottky and one-sided heterojunction diodes.^{25,26} It is understood that the SBH is spatially inhomogeneous^{27–29} and the SBH obtained from the $1/C^2$ - V characteristics corresponds to the barrier height averaged over the entire junction. In estimating the SBH from the current measurements, in contrast, the contribution of the lower-Schottky-barrier parts is more marked. The difference in SBH measured in the two methods was likely due to the spatial inhomogeneity of barrier height.

The turn-on voltage and SBH of Junction (A), which were close to those of Junction (C), were in disagreement with those of Junction (B). This implies that similarly to the case of ideality factors, the difference between these parameters was attributed to FAB irradiation; it is assumed that, by FAB irradiation, midgap states were formed on the surfaces of n-SiC layers and negative interface charges were produced as predicted using the charge-neutrality-level model.³⁰ Such negative interface charges were likely to play a role of increasing the SBH.

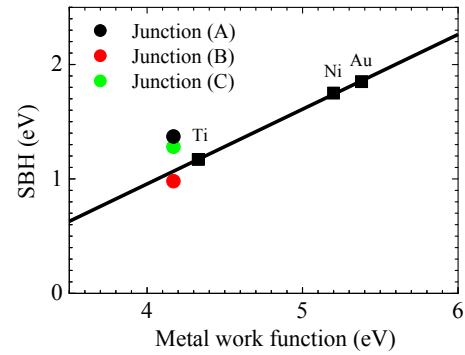


Fig. 9. (Color online) Dependence of SBH on metal work function.

We previously examined the effects of FAB irradiation energy on the electrical characteristics of Si Schottky diodes.³¹ The previously obtained results indicated that the SBH of n-Si Schottky diodes decreased with FAB irradiation, which was contrary to the variation in SBH observed for n-4H-SiC in the present work. The disagreement in the SBH trend between SiC and Si suggests that the features of interface states formed in the respective materials by FAB irradiation are different. Thus, systematic works using other metals are required.

The SBH of Junction (C) decreased owing to 400 °C annealing, although those of Junctions (A) and (B) increased. The changes in the SBHs of Junctions (B) and (C) qualitatively agreed with those in the turn-on voltages of the two junctions. The increase in the SBH of Junction (A) due to annealing disagreed with the behavior of its turn-on voltage. Such complicated changes in SBH might be related to the possible variations in both the density of states and the charge neutrality level due to annealing.

A reported relationship³² between the SBHs and work functions of Ti, Ni, and Au deposited on the Si faces of 4H-SiC layers is shown in Fig. 9. The results obtained from the $1/C^2$ - V characteristics of junctions after 400 °C annealing are also shown in this figure. We find that the SBH of Junction (B) agrees with the trend of the other metals, although the SBHs of Junctions (A) and (C) deviate from it. This result also supports the view that additional negative charges were formed at the interfaces of Junctions (A) and (C).

The larger ideality factor for Junction (A) than for Junction (B) suggests that the characteristics of Schottky diodes fabricated by SAB are not comparable to those of Schottky diodes prepared by conventional methods. Consequently, the conditions of SAB and the process after SAB should be optimized so as to realize Schottky diodes with acceptable characteristics.

5. Conclusions

We fabricated 17- μ m-thick Al foil/n-4H-SiC junctions by SAB. Their electrical properties were compared with those of Al/SiC Schottky junctions fabricated by evaporating Al films. Junctions fabricated by Al evaporation after irradiating SiC surfaces with the FAB of Ar were also characterized. We observed Schottky-like features in all of the fabricated junctions. The SBH of junctions with the irradiated SiC surfaces was larger than that of junctions fabricated without FAB irradiation and did not agree with the SBH trends of

other metals evaporated on SiC. These results were explained by considering the negative charges introduced at the surfaces SiC when they were irradiated with the Ar FAB. We also found that the ideality factors of junctions were degraded by FAB irradiation and were slightly recovered by annealing. The results suggested that SAB and post-bonding should be optimized.

Acknowledgment

This work was partially supported by the Matching Planner programs of JST.

- 1) J. B. Casady and R. W. Johnson, *Solid-State Electron.* **39**, 1409 (1996).
- 2) M. Bakowski, U. Gustafsson, and U. Lindefelt, *Phys. Status Solidi A* **162**, 421 (1997).
- 3) H. Okumura, *Jpn. J. Appl. Phys.* **45**, 7565 (2006).
- 4) J. Jiu, H. Zhang, S. Koga, S. Nagao, Y. Izumi, and K. Suganuma, *J. Mater. Sci.: Mater. Electron.* **26**, 7183 (2015).
- 5) J. Jiu, H. Zhang, S. Nagao, T. Sugahara, N. Kagami, Y. Suzuki, Y. Akai, and K. Suganuma, *J. Mater. Sci.* **51**, 3422 (2016).
- 6) H. Zhang, S. Nagao, K. Suganuma, H. J. Albrecht, and K. Wilke, *J. Mater. Sci.: Mater. Electron.* **27**, 1337 (2016).
- 7) A. Drevin-Bazin, F. Lacroix, and J.-F. Barbot, *J. Electron. Mater.* **43**, 695 (2014).
- 8) B. S. Passmore and A. B. Lostetter, Int. Workshop Integrated Power Packaging, 2017 [DOI: [10.1109/IWIPP.2017.7936763](https://doi.org/10.1109/IWIPP.2017.7936763)].
- 9) Y. Takahashi, H. Nogawa, A. Morozumi, and Y. Nishimura, IEEE CPMT Symp. Japan, 2016 [DOI: [10.1109/ICSI.2016.7801243](https://doi.org/10.1109/ICSI.2016.7801243)].
- 10) H. Takagi, K. Kikuchi, R. Maeda, T. R. Chung, and T. Suga, *Appl. Phys. Lett.* **68**, 2222 (1996).
- 11) H. Takagi, R. Maeda, N. Hosoda, and T. Suga, *Jpn. J. Appl. Phys.* **38**, 1589 (1999).
- 12) S. Essig, J. Benick, M. Schachtner, A. Wekkeli, M. Hermle, and F. Dimroth, *IEEE J. Photovoltaics* **5**, 977 (2015).
- 13) S. Essig and F. Dimroth, *ECS J. Solid State Sci. Technol.* **2**, Q178 (2013).
- 14) T. Suga, Y. Takahashi, H. Takagi, Y. Ishida, G. Gibbesch, and G. Ellsner, *Acta Metall. Mater.* **40**, S133 (1992).
- 15) T. Akatsu, N. Hosoda, and T. Suga, *J. Mater. Sci.* **34**, 4133 (1999).
- 16) A. Shigetou, T. Itoh, and T. Suga, *J. Mater. Sci.* **40**, 3149 (2005).
- 17) J. Utsumi and Y. Ichiyangi, *AIP Conf. Proc.* **1585**, 102 (2014).
- 18) S. Nishida, J. Liang, T. Hayashi, M. Arai, and N. Shigekawa, *Jpn. J. Appl. Phys.* **54**, 030210 (2015).
- 19) J. Liang, S. Nishida, M. Arai, and N. Shigekawa, *J. Appl. Phys.* **120**, 034504 (2016).
- 20) T. Suga, Y. Ishii, and N. Hosoda, *IEICE Trans. Electron.* **E80-C**, 297 (1997).
- 21) N. Shigekawa and J. Liang, *Proc. Int. Conf. Electronics Packaging*, 2017, p. 229.
- 22) J. Liang, S. Shimizu, S. Nishida, N. Shigekawa, and M. Arai, *ECS Solid State Lett.* **4**, Q55 (2015).
- 23) J. Liang, K. Furuna, M. Matsubara, M. Dhamrin, Y. Nishio, and N. Shigekawa, *ECS Trans.* **75** [9], 25 (2016).
- 24) S. Morita, J. Liang, M. Matsubara, M. Dhamrin, Y. Nishio, and N. Shigekawa, *Int. Workshop Low Temperature Bonding for 3D Integration*, 2017, p. 68.
- 25) C. Raynaud, K. Isoird, M. Lazar, C. M. Johnson, and N. Wright, *J. Appl. Phys.* **91**, 9841 (2002).
- 26) P. M. Gammon, A. Perez-Tomas, V. A. Shah, G. J. Roberts, M. R. Jennings, J. A. Covington, and P. A. Mawby, *J. Appl. Phys.* **106**, 093708 (2009).
- 27) J. H. Werner and H. H. Guttler, *J. Appl. Phys.* **69**, 1522 (1991).
- 28) R. T. Tung, *Phys. Rev. B* **45**, 13509 (1992).
- 29) D. Defives, O. Noblanc, C. Dua, C. Brylinski, M. Barthula, V. A. Fortuna, and F. Meyer, *IEEE Trans. Electron Devices* **46**, 449 (1999).
- 30) M. Morimoto, J. Liang, S. Nishida, and N. Shigekawa, *Jpn. J. Appl. Phys.* **54**, 030212 (2015).
- 31) S. Hisamoto, J. Liang, and N. Shigekawa, *IEEE Int. Meet. Future of Electron Devices*, 2016, p. 40.
- 32) A. Itoh and H. Matsunami, *Phys. Status Solidi A* **162**, 389 (1997).